Available online at www.sciencedirect.com
ScienceDirect
Journal of Power Sources 160 (2006) 1355–1360
JOURNAL OF POWER SOURCES
www.elsevier.com/locate/jpowsour

Compounds in solid electrolyte interface (SEI) on carbonaceous material charged in siloxane-based electrolyte

Hiroshi Nakahara [a,*], Steven Nutt [b]

[a] *Quallion LLC, Sylmar Biomedical Park, 12744 San Fernando Rd., Sylmar, CA 91342, USA*
[b] *Department of Materials Science and Engineering, University of Southern California, Los Angeles, CA 90089-0241, USA*

Received 5 February 2006; received in revised form 17 February 2006; accepted 24 February 2006
Available online 18 April 2006

Abstract

Microstructural characteristics of passive films on highly oriented pyrolytic graphite (HOPG) lithiated in siloxane-based electrolytes dissolving lithium bis(oxalato) borate (LiBOB) were analyzed. Scanning electron microscopy (SEM) images of the lithiated HOPG showed island-like deposition on the basal planes and film-like deposition on edge planes. X-ray spectroscopy revealed that the film-like deposition exhibited higher concentrations of Si and O than the island-like deposition. Fourier transformation infrared (FT-IR) spectroscopy of the siloxane-based electrolyte and the HOPG surface indicated consumption (decomposition) of LiBOB salt and bond breakage between the siloxane backbone and ethylene oxide side chain function groups. Based on FT-IR spectra from the lithiated graphite surface, the assigned function groups in the products included the flexible groups –Si–O– and –C–O–. These flexible function groups are expected to absorb the volumetric changes in graphite particles during lithiating and delithiating in an electrochemical cell, which will prevent continuous decomposition of siloxane electrolyte on the graphite surface.

Keywords: Lithium battery; Graphite; Siloxane; LiBOB; Passive film; Compounds

1. Introduction

Formation of the solid electrolyte interface (SEI) on graphite electrode surfaces in non-aqueous electrolytes (such as the ethylene carbonate/diethyl carbonate system) has been widely studied [1–13]. Exfoliation of graphene layers reportedly occurs during initial charging in propylene carbonate-based electrolytes because of co-intercalation of solvent [1,3]. Earlier studies asserted that the SEI film formed mainly by a solvent decomposition reaction, and that it was composed of $ROCO_2Li$ species, Li_2CO_3, and LiF [4–7]. Investigators subsequently concluded that the novel lithium salt, LiBOB, resulted in an SEI film that formed directly on graphite, rather than by a solvent decomposition reaction [14–16].

Polysiloxane-based electrolyte is a suitable candidate electrolyte for lithium battery systems because of the high conductivity relative to other polymer materials [17–21]. Polyethylene oxide (PEO) is a well-known solid polymer electrolyte that shows conductivity in the range of 10^{-6} to 10^{-7} S cm^{-1} [17–21]. By comparison, the conductivity of polysiloxane-based electrolyte exceeds this range by three orders of magnitude, reaching a value of approximately 10^{-3} S cm^{-1} [22]. Consequently, polysiloxane-based electrolyte has emerged as a primary candidate for the development of large lithium batteries for applications such as electric vehicles and other systems in which safety is a prime consideration [22].

SEI formation on graphite surfaces in polysiloxane-based electrolytes has been investigated in recent reports [23–28]. In one report, the existence of two types of passive film and associated morphological features were revealed by SEM observations [23,24]. One passive film was island-like and formed directly on the graphite surface, while the other was gel-like and covered the island-like film [23,24]. Further investigations have focused on modifications to improve lithium batteries. For instance, the addition of vinyl ethylene carbonate (VEC) to the polysiloxane-based electrolyte increased the discharge capacity of the graphite electrode and inhibited gel-like film formation, reducing the film resistance and charge transfer resistance [23,25]. In similar fashion, particular types of electrolyte salt [26] and the molecular structure of siloxane [27] also affected passive film

* Corresponding author. Tel.: +1 818 833 2016; fax: +1 818 833 2001.
E-mail address: hiroshi@quallion.com (H. Nakahara).

0378-7753/$ – see front matter © 2006 Elsevier B.V. All rights reserved.
doi:10.1016/j.jpowsour.2006.02.088

formation and the electrochemical response of the passive films on graphite electrodes. These reports indicated that the electrochemical and morphological characteristics of passive films formed on the graphite electrode surface (when lithiated in a polysiloxane-based electrolyte) could be modified by optimizing the electrolyte, which is thus a promising path to commercialization. However, the decomposition routes of siloxane-based electrolyte on the graphite surface during lithiation and the molecular structures of products—critical factors for electrolyte optimisation—remain to be clarified.

In the present work, the compounds in passive films on the HOPG charged in a siloxane-based electrolyte are analyzed and identified. The surface morphology of the HOPG was observed by SEM, and the composition of the passive film was determined by energy dispersive X-ray spectroscopy (EDS). Furthermore, FT-IR spectroscopy was performed to identify the types of function group associated with the compound present in the passive film. Finally, the decomposition reaction route of siloxane-based electrolyte and the chemical formulas for the products are proposed.

2. Experimental

2.1. Siloxane synthesis methods

The siloxane was synthesized at the University of Wisconsin, and the molecular structure was confirmed by FT-IR and NMR (^{1}H, ^{13}C, and ^{29}Si) analyses [28–31]. The molecular structures of siloxane and LiBOB are shown in Fig. 1. No impurities were detectable in the siloxanes by FT-IR and NMR analyses. The synthesis methods used to prepare the siloxane are described below [28–31].

A dehydrogenation reaction was carried out to generate a siloxane. Pentamethyldisiloxane (20.0 g, Gelest Inc.) and tri(ethylene glycol) allyl methyl ether (34.1 g, distilled) were mixed in a three-necked 100 mL flask. To this mixture, 100 μL of Karstedt's catalyst (3 wt.% solution in xylene) was added, and the reaction solution was heated to 75 °C, then cooled to room temperature. Samples were collected, and the process of hydrosilylation was followed by ^{1}H NMR measurements. After completion of the reaction, the excess tri(ethylene glycol) allyl methyl ether and its isomers were removed by Kugelrohr distillation. The result was recovered as a yellowish/brown liquid, and was decolorized by activated charcoal in refluxing toluene. The purified product was obtained by vacuum distillation, and the structure was confirmed spectroscopically. Next, lithium bisoxalato borate (LiBOB; Chemetal GmbH) was dissolved in the siloxane to achieve a 0.8 M concentration, and both were liquids at room temperature. The siloxane viscosity was 3.8 cP at 25 °C [28]. The conductivity and viscosity of the siloxane-based electrolyte were 3.65×10^{-4} S cm^{-1} and 18 cP at 25 °C [28].

2.2. SEM observation and EDS analysis

Siloxane and LiBOB (Chemetall GmbH) dissolved to achieve a 0.8 M concentration, was used as an electrolyte and both were liquids at room temperature. A block of HOPG (2 mm × 2 mm × 1 mm) was used for the working electrode. Copper mesh was used as a current collector, and was sandwiched around the HOPG block electrode. The electrode was covered with a polyethylene porous separator, and lithium metal was pressed against a copper mesh and used as the counter electrode. The working electrode, counter electrode, separator, and electrolyte were packaged in an aluminum laminated bag that was heat-sealed. The laminated cell was charged to 0.02 V. The charged electrode was removed from the disassembled cell in a glove box filled with Ar gas and a dew-point maintained below −75 °C, rinsed with diethyl carbonate (DEC), and dried under vacuum at room temperature. The surfaces of the HOPG were examined by SEM (JEOL JSM-5910LV) after a sputter coating with gold. In addition, the composition of the surface films on the specimens was analyzed by EDS (Oxford Instruments, EDS INCAEnergy 7274).

2.3. FT-IR measurements

The charged electrochemical cells described above were disassembled in a glove box filled with argon gas, and the dew-point was maintained below −75 °C. The HOPG was removed from the cells, rinsed with DEC, and dried under vacuum at room temperature. FT-IR measurements were carried out using a spectrometer (Perkin-Elmer Inc., Spectrum One FT-IR spectrometer) installed in a glove-box filled with argon and a dew-point maintained below −75 °C. Electrolyte was squeezed out from a separator, and the FT-IR spectra were measured. In addition, FT-IR spectra were acquired from the unused electrolyte to detect any impurities generated by chemical decomposition. This electrolyte was stored in a polypropylene bottle in a glove-box until other sample electrolyte taken from test cells was prepared.

3. Results

3.1. Microanalysis of films

SEM images of the HOPG blocks are shown in Fig. 2. The image of the pristine HOPG clearly shows the basal and edge

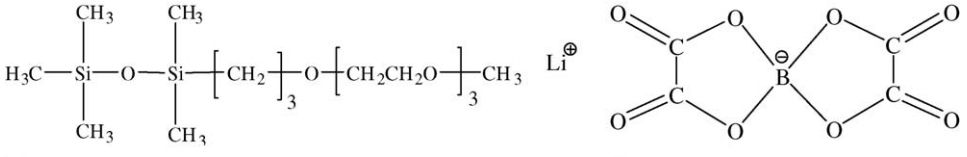

Fig. 1. Molecular structures of (a) siloxane molecule and (b) LiBOB.

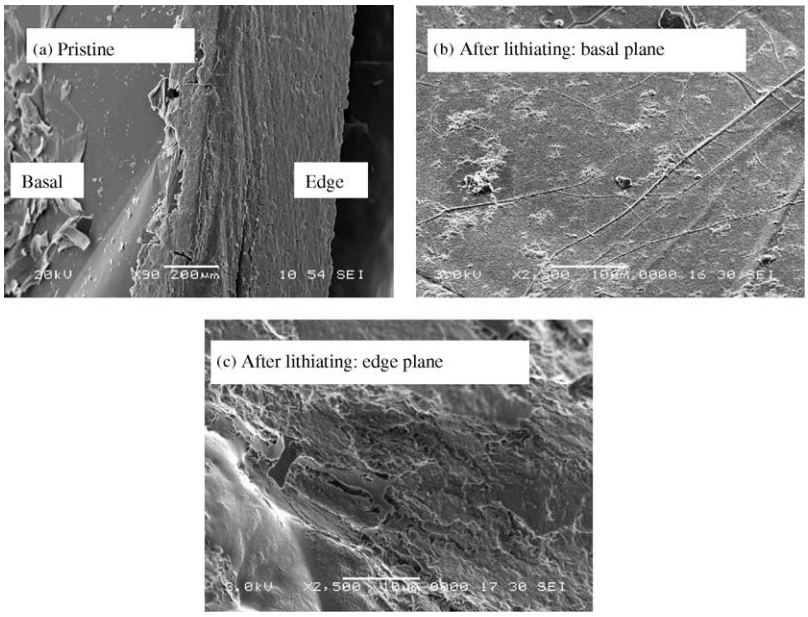

Fig. 2. SEM images of HOPG blocks: (a) pristine; (b) basal plane charged at 0.02 V vs. Li/Li$^+$, in siloxane-based electrolyte containing LiBOB; (c) edge plane charged at 0.02 V.

planes (Fig. 2a). Island-like deposition was observed on the basal plane of the lithiated HOPG in Fig. 2b. On the edge plane of the lithiated HOPG, the deposited film covered the surface (Fig. 2c).

Compositions of the surface films on the HOPG basal and edge planes were analyzed by EDS, the results of which are summarized in Table 1. Carbon was the primary element detected, and the silicon concentration on the basal plane was 0.1 at.%. On edge planes, silicon concentrations were higher relative to those on the basal plane.

3.2. FT-IR spectroscopy

Fig. 3 shows IR spectra acquired from (a) the siloxane-based electrolyte (removed from a test cell after lithiating HOPG) and (b) the unused electrolyte that was stored in a polypropylene bottle in a glove-box (gray curve). All peak positions were unchanged by lithiating HOPG. However, the absorption of IR for particular peaks (at 1091, 1197, 1272, 1294, 1348, 1779, and 1804 cm^{-1}) decreased after lithiating. The peak positions showing the decrease in IR absorption and the assigned function groups are summarized in Table 2. All peaks showing decreased absorption are attributed to LiBOB salt.

IR spectra of the HOPG surfaces for the pristine and the lithiated one are shown in Fig. 4. For the pristine HOPG, there was no absorption peak. Distinctive peaks were observed in the spectrum for the lithiated HOPG, and these peak positions are summarized in Table 3. These peaks are assigned to the function groups in a siloxane molecule, a LiBOB salt, and ones in derivatives of those species.

Table 1
Atomic composition on the surface of HOPG lithiated in siloxane-based electrolyte (EDS analysis result)

	C, at.%	O, at.%	Si, at.%
Basal plane	96.6	3.3	0.1
Edge plane	79.4	18.9	1.7

Table 2
Peak positions showing different peak height between the electrolyte taken from test cell and the unused one in the FT-IR spectrum for the siloxane-based electrolytes (Fig. 3) and the assigned function groups

Peak position (cm^{-1})	Assigned function groups
1091	>B–O–
1197	COOR
1272	COOR
1294	–COOR
1348	Li–O
1779	C=O
1804	C=O

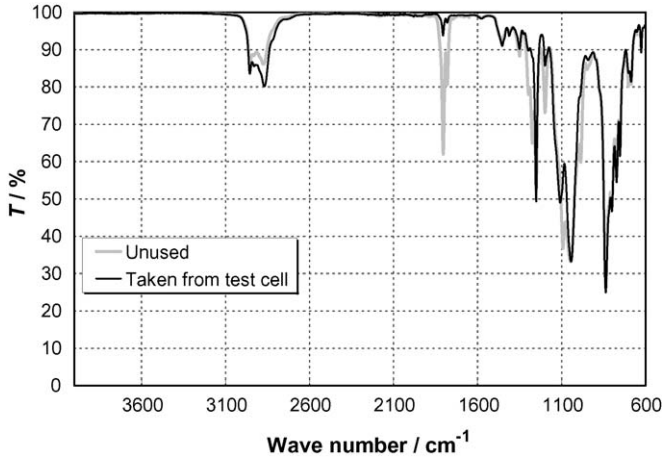

Fig. 3. FT-IR spectra for siloxane-based electrolytes.

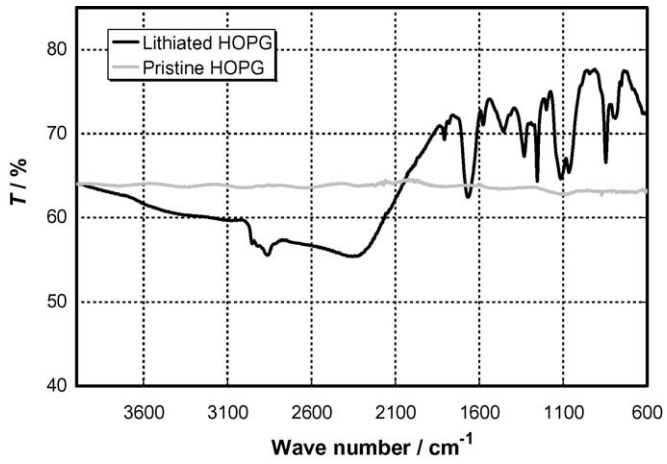

Fig. 4. FT-IR spectra for the pristine and the charged HOPG blocks.

Table 3
Peak positions in the FT-IR spectrum for HOPG block charged in siloxane-based electrolyte (Fig. 4), the assigned function groups and the possible source materials

Peak position (cm^{-1})	Assigned function groups	Possible source material
610	**–CH=CH$_2$, >C=CH$_2$**	**Siloxane**, **derivative**
678	**–CH=CH$_2$, >C=CH$_2$**	**Siloxane**, **derivative**
751	–CH$_2$–	Siloxane
784	SiCH$_3$	Siloxane
843	SiCH$_3$	Siloxane
923	**SiH**	**Siloxane**, **derivative**
984	**C=C**	**Siloxane** or **LiBOB**, **derivative**
1059	SiOR (SiOSi)	Siloxane
1108	SiOR (SiOSi), >B–O–, C–O	Siloxane or LiBOB
1196	–COOR	LiBOB
1253	–COOR	LiBOB
1328	SiCH$_3$, **Li–O**	**Siloxane** or **LiBOB**, **derivative**
1449	SiCH$_3$	Siloxane
1572	**–COO$^-$**	**LiBOB**, **derivative**
1657	**–CH=CH$_2$, >C=CH$_2$**	**Siloxane**, **derivative**
1774	C=O	LiBOB
1804	C=O	LiBOB
2343	**SiH**	**Siloxane**, **derivative**
2850	–CH$_2$–	Siloxane
2909	–CH$_3$	Siloxane
2941	–CH$_3$	Siloxane

Bold-face type shows the function groups in the derivatives of siloxane or LiBOB in table.

4. Discussion

SEM images of the HOPG surface indicated that an island-like film was deposited during lithiation in the siloxane-based electrolyte, and no gel-like film formed (Fig. 2b and c) [23–27]. SEM images revealed that the island-like deposit formed only on the basal plane (Fig. 2b), while on the edge plane, a film-like substance formed that was distinct from the film observed on the basal plane (Fig. 2c). These materials were generated by decomposition of the siloxane-based electrolyte [23–27]. In addition, EDS spectra (Table 1) revealed that the concentration of Si and O on edge planes was significantly higher than on basal planes. These observations support the assertion that decomposition of siloxane-based electrolyte occurred preferentially on edge planes rather than on basal planes. This assertion is consistent with the general perception that ROCO$_2$Li species, Li$_2$CO$_3$, and LiF are often involved in SEI formation on carbonaceous anodes lithiated in conventional carbonate based electrolyte [1–13].

Peak intensities in the spectra of siloxane-based electrolyte taken from the charged cell are smaller than those from the unused electrolyte (Fig. 3). As reported previously, the IR spectrum of siloxane-based electrolyte removed from the cell after charging (delithiating) lithium transition metal oxide was an exact replicate of the spectrum from the unused electrolyte [32,33]. Thus, the difference in IR spectra from the used and the unused siloxane-based electrolyte in case of lithiating carbonaceous material is notable (Fig. 3). The peaks that decreased in intensity after lithiating HOPG are attributed to the function groups in LiBOB salt, as listed in Table 2. Some peaks were assigned to function groups in the siloxane molecule, such as SiOR at 1091 cm^{-1} and SiCH$_3$ at 1348 cm^{-1}. However, these peak assignments are tentative because the characteristic peaks expected in other wave number ranges for these function groups were notably absent. Thus, the IR spectra of siloxane-based electrolytes shown in Fig. 3 suggest the consumption (decomposition) of LiBOB salt in siloxane-based electrolyte during lithiating HOPG. This finding is consistent with previous reports that suggested that LiBOB salt decomposed during initial lithiation of graphite (more than carbonate electrolyte solvent) [14–16].

IR spectra of the HOPG surface lithiated in siloxane-based electrolyte showed distinct differences from the pristine HOPG spectrum (Fig. 4). All peaks were assigned to function groups in the siloxane molecule, a LiBOB salt, and derivatives of those (Table 3). The function groups in the derivatives, shown in Table 3, are instrumental in determining the decomposition reaction route of siloxane-based electrolyte during lithiating HOPG. These groups include –CH=CH$_2$ or >C=CH$_2$ (610, 678, 1657 cm^{-1}), C=C (984 cm^{-1}), SiH (923, 2343 cm^{-1}), and Li–O (1328 cm^{-1}) for the derivatives from a siloxane molecule, and C=C (984 cm^{-1}), –COO$^-$ (1572 cm^{-1}), and Li–O (1328 cm^{-1}) for the LiBOB salt. In addition, the original function groups in the siloxane molecule and the LiBOB also were detected. From the siloxane molecule, these include SiOR or SiOSi in a backbone group (1059, 1108 cm^{-1}), CH$_3$ or SiCH$_3$ in a backbone group (784, 843, 1328, 1449, 2909, 2941 cm^{-1}), C–O in an ethylene oxide side chain group (1108 cm^{-1}), and –CH$_2$– in an ethylene oxide group (751, 2850 cm^{-1}). From a LiBOB salt, these include –COOR (1196, 1253 cm^{-1}), C=O (1774, 1804 cm^{-1}), >B–O–(1108 cm^{-1}), and Li–O (1328 cm^{-1}). These function groups were not affected by the lithiation of HOPG, and were retained in the products deposited on the HOPG surface.

Previous reports concluded that the SEI film was composed of ROCO$_2$Li species, Li$_2$CO$_3$, and LiF, all of which were produced by the decomposition of carbonate-based electrolyte, and

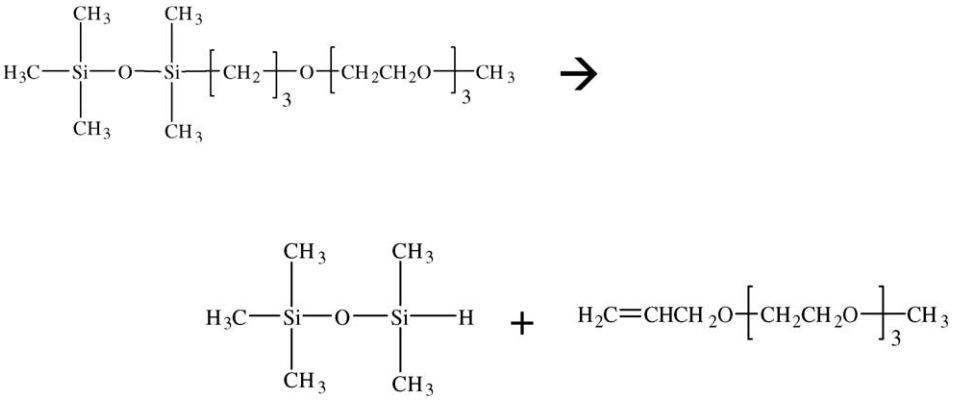

Fig. 5. Decomposition reaction of a siloxane molecule on HOPG surface during lithiating HOPG.

are derivatives of the carbonate solvents and the electrolyte salt [4–7]. Based on these and other reports [4–7,24–28,33] as well as the present evaluation results of HOPG surface, a proposed reaction route for siloxane-based electrolyte decomposition is shown in Fig. 5, along with the molecular structure of products. Regarding the decomposition reaction of a siloxane molecule, given the function groups above, the siloxane backbone and ether group (in ethylene oxide side chain group) remain in the products after decomposition reaction. Function groups such as SiH and –CH=CH_2 or >C=CH_2 in products suggest the breakage of Si–C bonds between the siloxane backbone and the ether side chain group (refer to the siloxane molecular structure shown in Fig. 1a). In addition, there is a possibility of bond breakage of the ether group to produce Li–O bonds in a further decomposition reaction, although the source is not yet clarified in this work. We assert that the compounds shown in Fig. 5 are products of siloxane molecule decomposition. Furthermore, regarding LiBOB decomposition, the presence of function groups $–COO^-$ and Li–O indicate the breakage of B–O bonds in a bis(oxalato) borate anion (refer to the LiBOB molecular structure in Fig. 1b). This assertion is consistent with other reports [14–16], although the absorption peaks for B–O were also detected (Table 3).

The present observations provide insight into results of long-term tests of battery performance, such as cycling and calendar life with electrochemical cells containing a siloxane-based electrolyte. Different types of siloxane molecules were evaluated as electrolytes in lithium secondary electrochemical cells (lithium transition metal oxide cathode and graphite anode) by cycling and calendar life [34]. The siloxane-based electrolyte used in the present study showed the greatest discharge capacity retention after long-term testing, including cycling and calendar life tests [34] Interpretations of test results led to two hypotheses–that the elastic passive film formed by the decomposition of siloxane-based electrolyte on the graphite surface, and that the superior passive film prevented siloxane-based electrolyte from continuous decomposition under long-term testing conditions. The present study provided additional insight into the compounds present in the passive film. In particular, these compounds appear to be comprised of –Si–O– bonds and/or –C–O– bonds that rotate in unconstrained fashion to absorb the volumetric change of graphite during charge–discharge cycling.

5. Conclusions

The passive film formed on a graphite electrode was characterized by using SEM, EDS, and FT-IR. The siloxane-based electrolyte generated island-like deposition on basal planes of HOPG and film-like deposition on edge planes. The film-like deposit contained higher concentrations of silicon and oxygen.

Chemical formulas for the products of the decomposition reaction of siloxane-based electrolyte were proposed. The passive film on the graphite electrode was composed of compounds containing flexible –Si–O– and –C–O– bonding. In the siloxane-based electrolyte, these elastic passive films prevent continuous decomposition of the siloxane electrolyte because the passive films prevent exposure of fresh graphite surface to siloxane-based electrolyte (normally occurring at the crack due to expansion and shrinkage of graphite particles during lithiation and delithiation). The long-term battery performance, such as cycle life and calendar life, is expected to be superior in batteries containing a siloxane-based electrolyte because of the formation of an elastic passive film on the graphite electrode. In future work, the present siloxane electrolyte will be modified with dissolving organo-borate salts and electrolyte additives, and the resulting battery performance will be investigated and developed for future use in the lithium battery industry.

Acknowledgements

Financial support from the U.S. Army's Communications–Electronics Research, Development and Engineering Center (CERDEC) is gratefully acknowledged. The University of Wisconsin is acknowledged for preparation of the siloxanes, and technical discussions with personnel at Argonne National Laboratory are gratefully acknowledged.

References

[1] M. Inaba, Z. Shiroya, Y. Kawatate, A. Funabiki, Z. Ogumi, J. Power Sources 68 (2) (1997) 221–226.
[2] S.-K. Jeong, M. Inaba, Y. Iriyama, T. Abe, Z. Ogumi, Electrochim. Acta 47 (2002) 1975–1982.
[3] R. Mogi, Y. Inaba, T. Iriyama, Z. Abe, Ogumi, J. Power Sources 108 (2002) 163–173.

[4] D. Aurbach, E. Zinigrad, Y. Cohen, H. Teller, Solid State Ionics 148 (2002) 405–416.
[5] D. Aurbach, I. Weissman, A. Zaban, P. Dan, Electrochim. Acta 45 (1999) 1135–1140.
[6] D. Aurbach, A. Zaban, Y. Gofer, Y.E. Ely, I. Weissman, O. Chusid, O. Abramson, J. Power Sources 54 (1995) 76–84.
[7] Z. Ogumi, A. Sano, M. Inaba, T. Abe, J. Power Sources 97/98 (2001) 156–158.
[8] A.M. Andersson, Dissertation for the Degree of Doctor of Philosophy, Uppsala University, 2001.
[9] G. Eichinger, J. Eletroanal. Chem. 74 (1976) 183.
[10] J.O. Besenhard, Carbon 14 (1976) 111.
[11] D. Aurbach, Nonaqueous Electrochemistry, Marcel Dekker, New York, 1999.
[12] D. Aurbach, A. Zaban, Y. Ein-Eli, I. Weissman, O. Chusid, B. Markovsky, M. Levi, A. Shechter, E. Granot, J. Power Sources 68 (1997) 91.
[13] M. Ue, M. Takeda, M. Takehara, S. Mori, J. Electrochem. Soc. 144 (1997) 2684.
[14] K. Xu, S. Zhang, B.A. Poese, T.R. Jow, Electrochem. Solid-State Lett. 5 (1) (2002) A259–A262.
[15] K. Xu, S. Zhang, T.R. Jow, W. Xu, C.A. Angell, Electrochem. Solid-State Lett. 5 (1) (2002) A26–A29.
[16] K. Xu, S. Zhang, T.R. Jow, Electrochem. Solid-State Lett. 6 (6) (2003) A117–A120.
[17] Y. Kang, W. Lee, D.H. Suh, C. Lee, J. Power Sources 119–121 (2003) 448–453.
[18] I.J. Lee, G.S. Song, W.S. Lee, C. Lee, J. Power Sources 114 (2003) 320–329.
[19] M. Shibata, T. Kobayashi, R. Yosomiya, M. Seki, Eur. Polym. J. 36 (2000) 485–490.
[20] Z. Zhang, S. Fang, Electrochim. Acta 45 (2000) 2131–2138.
[21] Z. Wang, M. Ikeda, N. Hirata, M. Kubo, T. Ito, O. Yamamoto, J. Electrochem. Soc. 146 (6) (1999) 2209–2215.
[22] B. Oh, D. Vissers, Z. Zhang, R. West, H. Tsukamoto, K. Amine, J. Power Sources 119–121 (2003) 442–447.
[23] H. Nakahara, A. Masias, S.Y. Yoon, T. Koike, K. Takeya, Proceedings of the 41st Power Sources Conference, June 14–17, Philadelphia, 2004, p. 165.
[24] H. Nakahara, S.Y. Yoon, T. Piao, S. Nutt, F. Mansfeld, J. Power Sources 158 (2006) 591–599.
[25] H. Nakahara, S.Y. Yoon, S. Nutt, J. Power Sources, in press.
[26] H. Nakahara, S. Nutt, J. Power Sources 158 (2006) 1386–1393.
[27] H. Nakahara, S.Y. Yoon, S. Nutt, J. Power Sources, in press.
[28] H. Nakahara, Study of passive film formation on graphite surface in polysiloxane-based electrolyte for the application of Li secondary battery, PhD dissertation, University of Southern California, 2006.
[29] R. Hooper, L.J. Lyons, M.K. Mapes, D. Shumacher, D.A. Moline, R. West, Macromolecules 34 (2001) 931.
[30] Z. Zhang, D. Sherlock, R. West, K. Amine, L.J. Lyons, Macromolecules 36 (2003) 9176.
[31] Z. Zhang, N. Rossi, K. Lyons, R. Amine, West, Polym. Preprints 45 (1) (2004) 700.
[32] M. Tanaka, H. Nakahara, S.Y. Yoon, H. Tsukamoto, S. Nutt, Proceedings of the 208th ECS Meeting, Los Angeles, 2005 (D2-0719P).
[33] H. Nakahara, S.Y. Yoon, M. Tanaka, S. Nutt, J. Power Sources 160 (2006) 645–650.
[34] S.-Y. Yoon, H. Nakahara, Z. Zhang, Q. Wang, K. Amine, R. West, H. Tsukamoto, Proceedings of the Second International Conference on Polymer Batteries and Fuel cells, June 12–17, Las Vegas, USA, 2005 (Abstract No. 121).